

OPTIMIZED DESIGN OF UHPC BRIDGE DECK SLAB FOR HYBRID CABLE-STAYED GIRDER BRIDGE

Hoon-Hee Hwang*, Dong-Min Yoo*, Sung-Yong Park, Byung-Suk Kim****

**Technical & Research Division*

Korea Road & Transportation Association

5F, HanDo BLDG, #987-14, Daechi-3dong, Gangnam-gu, Seoul, Korea

poonhee@krta.co.kr

***Structural System Research Division*

Korea Institute of Construction and Technology

2311, Daewha-dong, ilsanseo-gu, Goyang-si, Gyeonggi-do, Korea

ABSTRACT

This research is a part of the comprehensive research project to develop the optimized UHPC(Ultra High Performance Concrete) precast bridge deck system applying to durable and cost-effective hybrid cable stayed bridge. It is required that the self-weight of superstructure decreases to realize durable and cost-effective hybrid cable stayed bridge. It is achieved to develop the technologies for light weight and durable bridge decks.

UHPC developed by KICT(Korea Institute of Construction and Technology) is an expectable structural material which has high strength and crack resistance. This research presents the design concept to develop high efficient section of UHPC bridge decks. Longitudinally prestressed ribbed section is proposed to make the best use of an advantage of UHPC.

1. INTRODUCTION

Ultra High Performance Concrete(UHPC hereinafter) is a attractive structural material with high strength and durability. These advantages of UHPC enable the design to attempt various efficient sections.

General reinforced concrete bridge deck slabs are composed of the parts in the form of plates with solid section. And appropriate amount of reinforcement is placed in accordance with bending design of a beam with unit width or empirical design method. Such deck slabs are designed to satisfy the minimum thickness regulated by Korea Highway Bridges Design Code (2005) (KHBDC hereinafter) to resist punching shear failure. As a result, it leads to a considerable amount of load that limits competitive design.

However, UHPC is a structural material with high performance, so that it can be achieved to construct slim and lightweight structural members with relatively small amount of material.

Hybrid cable stayed bridge(HyCAB hereinafter) being developed by Korea Institute of Construction and Technology(KICT hereinafter) needs a innovative bridge deck system to realize the improvement of the long-span bridges. A part of the study for development of UHPC precast bridge deck system which applying to HyCAB is summarized. The structural type of the UHPC precast bridge deck slabs is presented and the design concepts are established in this paper.

1. Structural type and design concept

1.1. Selection of structural type

The shape of UHPC bridge deck currently in application is being developed into various types of sections such as π - type or ribbed type to satisfy the required performance per each type of bridge. In this paper, the section type with prestressed ribs in longitudinal direction is presented to realize high performance as a innovative bridge deck system(Figure 1). The main direction of UHPC precast bridge deck slab section is longitudinal and prestressed ribs with pretention method are reinforced in same direction in order to maximize bending capacity.

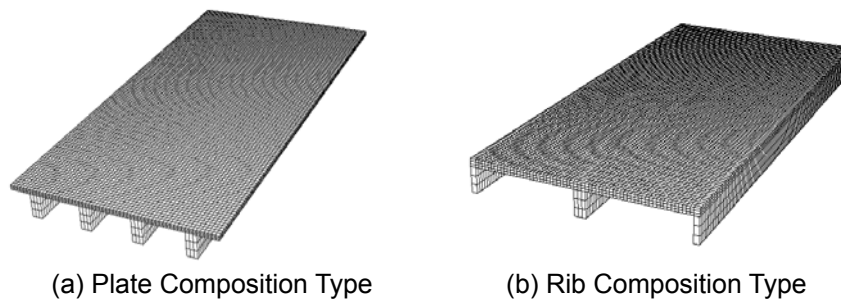


Figure 1. Recommended form of UHPC bridge deck slab

1.2. Establishment of Design Concept

UHPC bridge deck slabs should be designed according to the algorithm that decides each specification of section to satisfy the minimum requirement for preventing failure(Figure 2). Two kinds of failure modes are identified for the ribbed slab: local and global failures. Local failures comprise bending and punching-shear failure of thin slabs, while global failures are related to the loss of bending and shear resistance of prestressed T girders, representing a unit element of the ribbed slab(Spasojevic A., 2008)

Therefore, to decide each design variable of UHPC bridge deck slabs, local failure should be reviewed by deciding the minimum thickness requirement of plate in accordance with punching shear mechanism. Then the rib spacing is decided by drawing the correlation between plate thickness and rib spacing according to two-way bending behavior of plate. For global failure review, the one-way bending behavior of a T-beam that has effective width is analyzed to decide rib height and the amount of prestress.

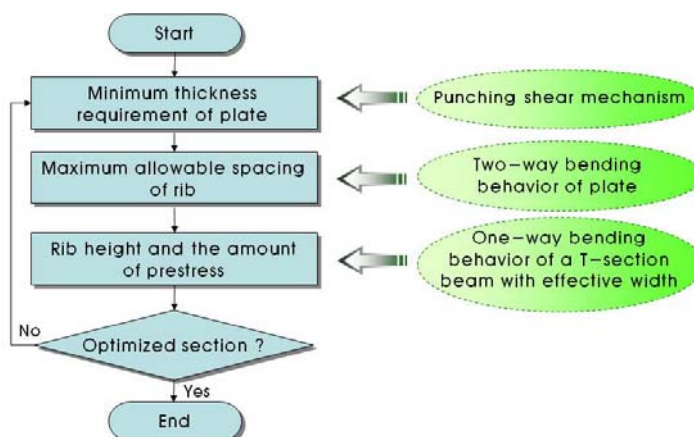


Figure 2. Algorithm for drawing the optimized section of UHPC bridge deck slabs

Ultimate Strength design for reinforced concrete member is performed according to the equivalent rectangular stress block model proposed by Whitney in case of using ordinary concrete. However, the purpose of the equivalent rectangular stress block model is to plan efficient design by simplifying stress-strain relationship of ordinary concrete in the form of parabola. Therefore, it is not appropriate to apply it to a case of UHPC that behaves similar to linear. Also, tensile strength of concrete is not generally considered in terms of practical strength design of reinforced concrete member, but the tensile performance is reinforced remarkably due to inclusion of steel fiber for UHPC so the tensile strength design model related to the contribution of steel fibers and the range of crack width limit should be developed or selected.

In this study, the material model proposed by Virginia Tech (Figure 4) which is known for its easy application and relatively accurate result and Maximum Crack Opening Criterion (AFGC, 2002) (Table 1) are adopted to calculate the bending capacity of the UHPC section.

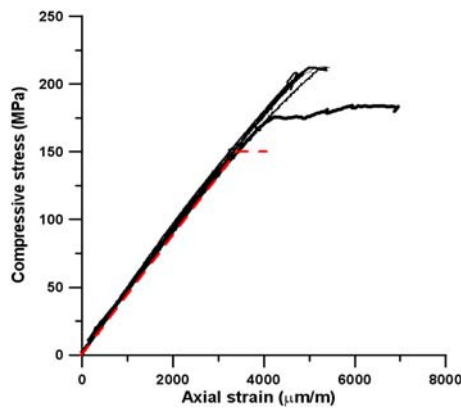


Figure 3. Stress-strain relationship of UHPC

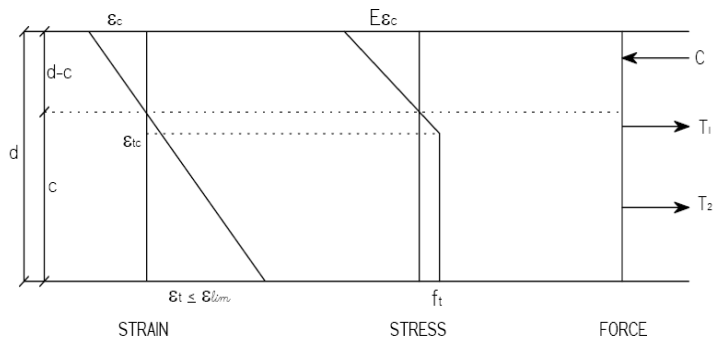


Figure 4. Study case of the U.S.A (Virginia Tech)

Table 1. Maximum Crack Opening Criterion (AFGC, 2002)

Limiting crack criterion		Remark
Unreinforced UHPC sections	$\omega_{lim} = 0.3 \text{ mm}$	ω_{lim} : Max. admissible crack opening L_f : fiber length
Reinforced UHPC sections	$\omega_{lim} = \min(L_f / 4, h / 100)$	
Limiting strain criterion		ε_{lim} : max. admissible strain
Unreinforced UHPC sections	$\varepsilon_{lim} < \omega_{lim} / l_c = 1.5\omega_{lim} / h$	l_c : characteristic length h : height of structure
Reinforced UHPC sections	$\varepsilon_{lim} < \omega_{lim} / l_c = \min(3L_f / 8h, 3 / 200)$	

2. Design of optimized section of UHPC bridge deck slab

2.1. Determination of the Plate Thickness

The thickness of plate members comprised in UHPC bridge deck slab must be thicker than the minimum requirement, which is required to prevent punching shear failure. Punching shear strength is affected by many variables such as concrete strength, loading area, boundary condition, thickness of member and etc. For the proposed UHPC bridge deck slab type, the variables except thickness have certain conditions so the punching shear strength was applied as a measure to decide the minimum

thickness requirement of the plate member. The punching shear mechanism of UHPC plate is similar to that of ordinary concrete bridge deck slab, but there might be some difference in strength development depending on the characteristic of matrix and steel fiber.

Here we have selected the most appropriate formula for UHPC by comparing six formulas proposed by former researchers and the experimental data of punching shear strength of UHPC plate. The compared formulas are proposed by Shaaban et al.(1994), Tan et al.(1994), breakout strength model(Fuchs et al., 1995), Ductal, ACI318-05(2005) and the general formula (Graddy et al., 2002). The comparison results showed that the general formula by Graddy (2002) predicted the most accurate experimental value for punching shear strength of UHPC that is performed by KICT(Figure 5(a)). ACI 318-05 (2005) is derived from same model with the general formula proposed by Graddy et al., but the angle of a failure plane is assumed 45 degrees to draw safe prediction(Figure 5(b)). Thus in this study we have applied ACI 318-05 (2005) to decide the thickness of plate that is required to prevent punching shear strength.

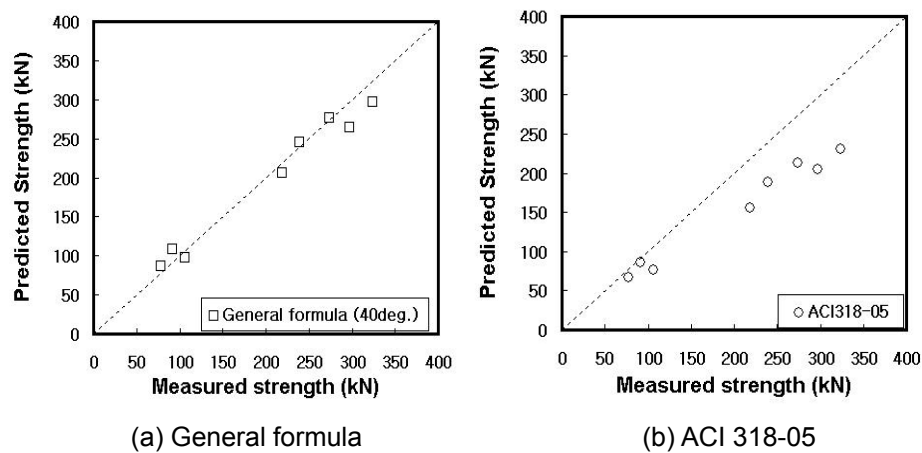


Figure 5. Comparison example of experimental and predicted value (punching shear strength)

On figure 5, the data along the diagonal line means the agreement between the experimental and predicted values. The data on the upper left of the diagonal line means that the predicted value calculated from the formula is greater than the experimental value. It shows a little bit of risky prediction tendency. The opposite case means that the calculated value by formula predict the punching shear strength safely.

Table 2. ACI 318-05 and the General formula by Graddy et al

ACI318-05 (2005)	General formula by Graddy et al(2002)
$V_c = \frac{1}{6} \left(1 + \frac{4}{\beta_c} \right) \sqrt{f_c} b_0 d$ $V_c = \frac{1}{12} \left(\frac{\alpha_s}{b_0 d} + 2 \right) \sqrt{f_c} b_0 d$ $V_c = \frac{1}{3} \sqrt{f_c} b_0 d$	$V_c = 2 \left(b_1 + b_2 + 2 \frac{\bar{d}}{\tan \theta} \right) \frac{\bar{d}}{\tan \theta} f_i$ <p>where, $f_i = \frac{1}{6} \left(1 + \frac{2}{\beta_c} \right) \sqrt{f_c}$ (MPa), b_1=Length of short edge of loading surface(mm), b_2=Length of long edge of loading surface (mm), \bar{b}=effective height (mm), θ=slope angle of failure plane, β_c=edge ratio of loading surface, f_c=Compressive strength of concrete</p>

Punching shear failure of bridge deck slab in service state is caused by accumulated fatigue due to repeated load and environmental factors. But fatigue and environmental factors are not considered in this paper because these are not studied sufficiently yet. So, only the predicted punching shear strength values by ACI 318-05 (the evaluating formula for static punching shear strength) is used. And as a result, the minimum thickness requirement of plate to prevent punching shear failure was set to be greater than 40mm as shown in Figure 6.

The estimated maximum value of load, which is multiplying the rear wheel load of DB-24 by impact coefficient and load factor in Korea Highway Bridge Design Code (KHBDC), is about 268kN. This value is similar to the maximum wheel load observed in Japan(1998).

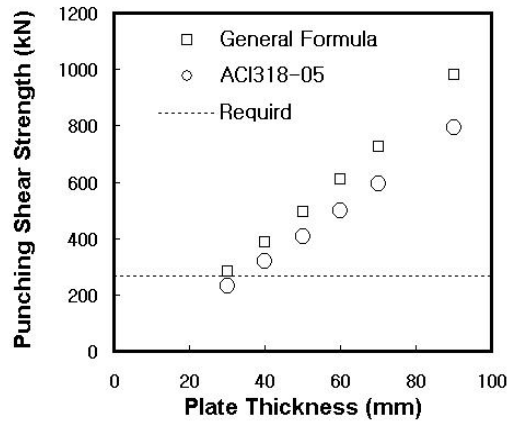
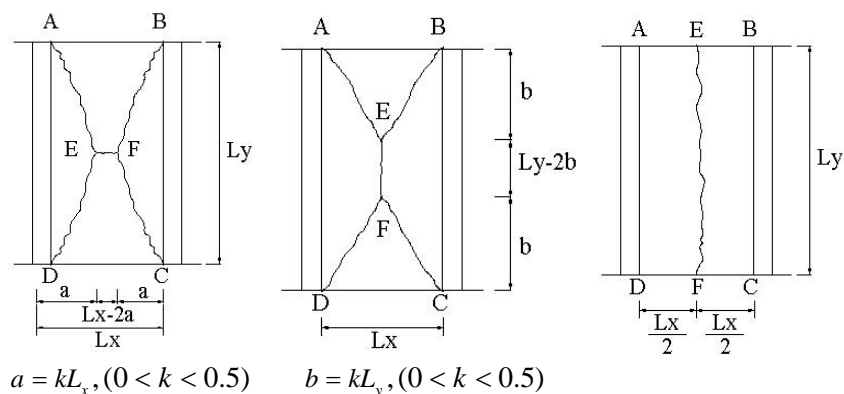


Figure 6. Minimum thickness requirement of plate member(punching shear behavior)

2.2. Determining Rib Spacing

Rib spacing can be determined by deriving the correlation between plate thickness and rib spacing through estimating two-way bending behavior, a form of local failure that occurs on plate member.

The strength for two-way bending of plate member can be estimated with the yield line theory. Estimation of failure load of member by yield line theory is appropriate but how the pattern of yield line is assumed has a huge influence on the accuracy. We considered three cases below in Figure 7 to determine rib spacing. Figure 7(a) and Figure 7(b) show a yield line in X shape caused by two-way bending behavior of plate member. Figure 7(c) shows one-way bending crack that is caused parallel to longitudinal direction in case where rib spacing is too wide or ribs are omitted in transverse direction.



(a) Case 1

(b) Case 2

(c) Case 3

Figure 7. Assumed Yield Line Pattern of UHPC Bridge Deck Slab

The correlation between plate thickness and rib spacing can be explained with the principle of virtual work for four plate members created by yield lines. The calculation process for case 2 is explained in this paper.

First, plate member is divided into four elements by the formation of yield line. Then we can apply the principle of virtual work to each element.

The internal virtual work (W_{int}) of each element is as shown in Table 3. Assuming that the virtual displacement of the central point is δ , the external virtual work (W_{ext}) is $P \cdot \delta$. In accordance with the principle of virtual work, $W_{int} = W_{ext}$ is established and since the plate member does not include reinforcing bar or tendon, $M_x = M_y$ is established as shown in Table 3. Thus, the formula for load P can be expressed as in equation (1).

Table 3. Internal virtual work for each element (Case 2)

Segment	Rotation angle, θ_x	Virtual work $M \cdot \theta \cdot L$	Segment	Rotation angle, θ_y	Virtual work $M \cdot \theta \cdot L$
AEFD	$\frac{2\delta}{L_x}$	$M_x \cdot \frac{2\delta}{L_x} \cdot L_y$	ABE	$\frac{\delta}{b}$	$M_y \cdot \frac{\delta}{b} \cdot L_x$
BCEF	$\frac{2\delta}{L_x}$	$M_x \cdot \frac{2\delta}{L_x} \cdot L_y$	CFD	$\frac{\delta}{b}$	$M_y \cdot \frac{\delta}{b} \cdot L_x$
Total	$4M_x \cdot \frac{L_y}{L_x} \cdot \delta + 2M_y \cdot \frac{L_x}{b} \cdot \delta$				

$$P = 2M \left(2 \frac{L_y}{L_x} + \frac{L_x}{b} \right) \quad (1)$$

From equation (1), rib spacing L_x and the equation for resisting moment of section according to KICT UHPC plate thickness can be expressed in a quadric equation shown in formula (2).

$$\frac{P}{2M} = \frac{2kL_y^2 + L_x^2}{kL_xL_y}, \quad L_x^2 - \frac{P}{2M} kL_yL_x + 2kL_y^2 = 0$$

$$\therefore L_x = \frac{-b \pm \sqrt{b^2 - 4ac}}{2a} \quad (2)$$

$$\text{where, } a = 1, \quad b = -\frac{P}{2M} kL_y, \quad c = 2kL_y^2$$

In formula (2), $P = 268\text{kN}$ (refer to 3.1), $L_y = 4000\text{mm}$, and $b = kL_y$ (predicted progressive length if initial crack occurs in longitudinal direction; $0 < b < 0.5L_y$) are substituted to express the equation in a formula for rib spacing L_x and resisting moment of section M .

The value of resisting moment of section, M is depending on the plate thickness and it is calculated by applying Maximum Crack Opening Criterion (AFGC, 2002) in Table 1 and material model of Virginia Tech shown in Figure 4.

The correlation between rib spacing and plate thickness was derived through the above process. The correlation in accordance with the changing k value was shown in Figure 8 (a) for case 2. The

correlation between rib spacing and plate thickness for case 2 and 3 were derived by using the same method and the results are shown in Figure 8 (b). The result for case 1 and 2 are the same because the same yield line in X shape is created when coefficient $k = 0.5$.

We decided that establishment of correlation in consideration of crack forms that occurs in service state is necessary for more economic and detailed design; thus various patterns of yield lines were reviewed. However, when deriving the correlation between plate thickness and rib spacing without any experience in detailed analysis or experiment, it would be safer to determine by comparing the worst case in every possible condition. In that sense, if 40mm is applied as the plate thickness to prevent punching shear failure the maximum allowable rib spacing is 500mm as shown in Figure 8 (b).

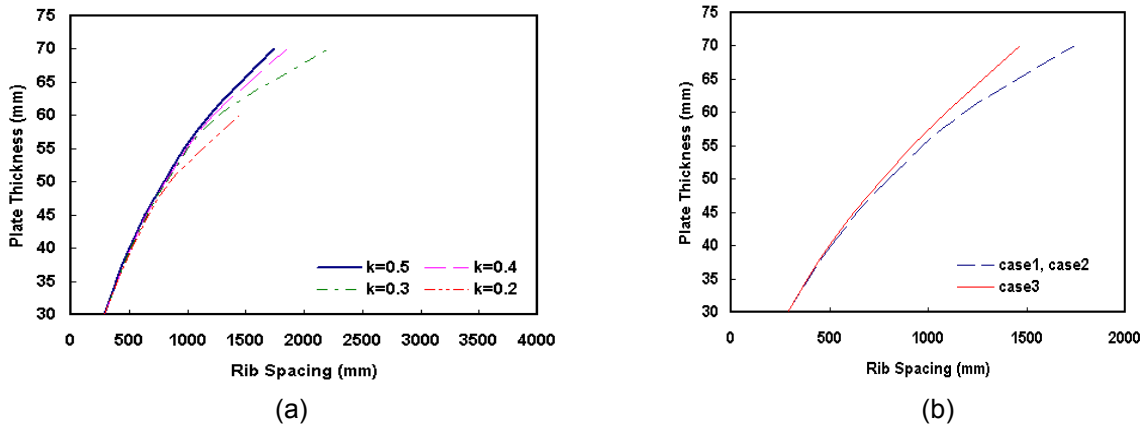


Figure 8. Correlation between rib spacing and plate thickness

3.3 Determination of rib specifications and number of tendon

The height of ribs and the amount of prestress were determined according to the design procedure of T-beam in the perspective of the whole structure. In this case, so the plate members work as a compressed flange that the concept of effective width considered with actual stress distribution was introduced. The effective width was calculated according to the equation (3) stipulated in the AASHTO LRFD Bridge Design Specifications(2007).

$$\min\left(\frac{L}{4}, 12t + b_w, B\right) \quad (3)$$

In this study, following values were applied to compute an effective width. “ L ”(the longitudinal length of a segment or the distance between cross beams) is 4000 mm, “ t ”(the plate thickness as calculated in 3.1) is 40 mm, “ B ” (the rib spacing as calculated in 3.2) is 500 mm and “ b_w ” (rib width) is 100 mm. Although there was a case in which 70 mm was applied to rib width(b_w) considering the cover and diameter of tendon(Toutlemonde et al, 2005), 100mm was assumed in this study taking account of double reinforcement of tendon and post-tension.

Meanwhile, as the required minimum thickness of plate members was estimated by the static equation for punching shear strength, safer choice is needed to be made considered with faster fretting from fatigue and corrosion. Therefore, 50mm and 60 mm were included in the plate thickness, separate from the minimum thickness of 40 mm. Table 4 shows rib spacing and effective width in accordance with plate thickness.

Table 4. Rib spacing and effective width in accordance with plate thickness

Plate thickness(mm)	Rib spacing(mm)	Effective width(mm)
40	500	500
50	700	700
60	1000	820

The amount of prestress for effective sections of plate members shown on Table 4 varies depending on rib height. Thus, we conducted a first level finite element analysis with various rib height to calculate the maximum tensile stress on the bottom of ribs. To introduce prestress offsetting this tensile stress, we computed the required number of tendon based on allowable stress design.

In the second level finite element analysis, we reviewed deflection by using models including tendons that can be actually placed.

We assumed that tendon of 15.2mm diameter SWPC7B was placed in a straight line for the purpose of convenience convenience in construction and we reviewed two cases where we placed tendons on the lower part only and where we placed them lower and upper parts of the section.

To determine the amount of prestress, we considered tensile capacity of UHPC and did not allow cracking as substantive research on core technology including setting and controlling of cracking would be required in case we allowed cracking.

For loads, wheel load of DB-24 truck multiplied by impact coefficient was applied as live load and 80 mm thick asphalt pavement with the weight of UHPC was considered as dead load. The unit weight of the asphalt pavement and UHPC are $23.0 \text{ kN} / \text{m}^3$ and $25.5 \text{ kN} / \text{m}^3$ respectively.

Figure 9 shows the examples of finite element analysis model and Table 5 summarizes the results of the finite element analysis. In the names of analysis model in Table 5, 'S00' represents plate thickness, 'TR000' rib height, 'P0' placement of tendon ('P1' means on the lower part only and 'P2' means on the lower and upper parts), and 'L' represents load case in which both dead load and live load are applied.

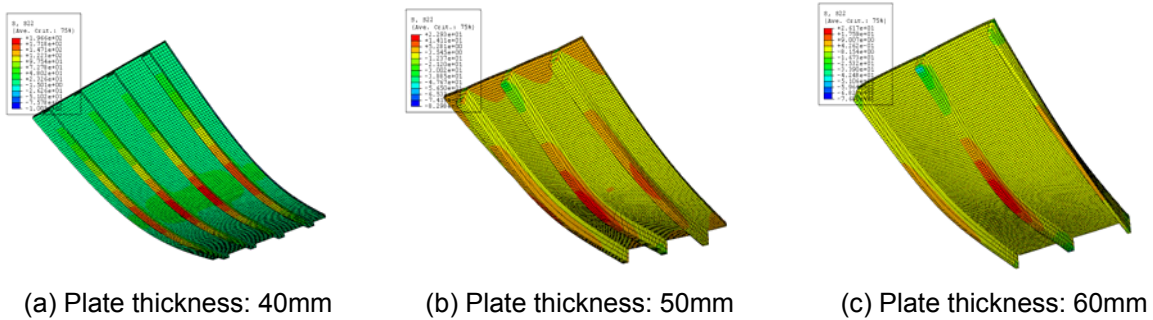
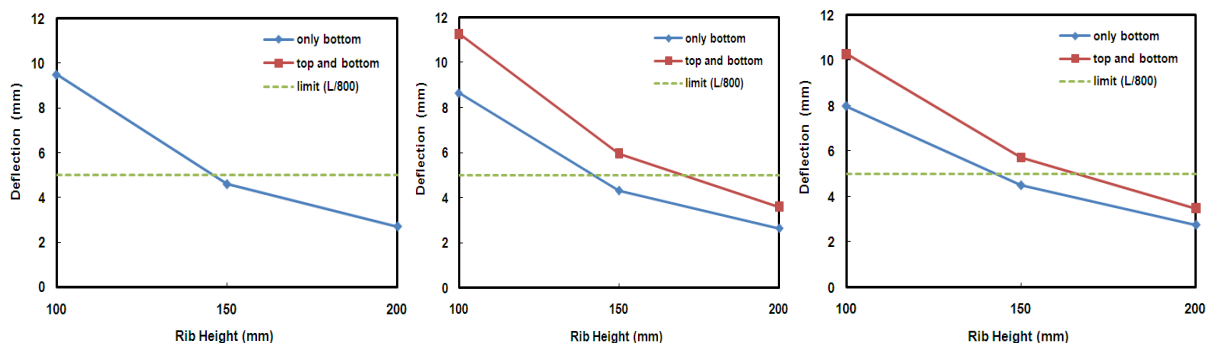


Figure 9. Contour of tensile stress by finite element analysis

Table 5. Rib height and required number of tendon

Analysis model	Specification (mm)			Number of tendon		Deflection (mm)	Remarks (serviceability check)	
	Plate thickness	Rib height	Rib number (Spacing)	Required quantity	Used quantity			
S40TR100P1L	40	100	4 (500)	1.7	2	9.50	NG	
S40TR100P2L				2.6	4	60.0	NG	
S40TR150P1L		150		1.3	2	4.60	OK	
S40TR150P2L				1.8	2	28.3	NG	
S40TR200P1L		200		200	1.1	2	2.71	OK
S40TR200P2L					1.4	2	21.0	NG
S50TR100P1L	50	100	3 (700)	2	2	8.65	NG	
S50TR100P2L				3.2	4	11.3	NG	
S50TR150P1L		150		1.5	2	4.32	OK	
S50TR150P2L				2.1	3	5.96	NG	
S50TR200P1L		200		200	1.3	2	2.64	OK
S50TR200P2L					1.7	2	3.60	OK
S60TR100P1L	60	100	2 (1000)	2.4	3	7.99	NG	
S60TR100P2L				3.7	4	3.49	OK	
S60TR150P1L		150		1.8	2	4.51	OK	
S60TR150P2L				2.7	4	5.73	NG	
S60TR200P1L		200		200	1.5	2	2.77	OK
S60TR200P2L					2	2	3.48	OK

Figure 10 shows changes of deflection in accordance with rib height when plate thickness is constant. In order to satisfy the deflection standards of KHBDC(Korea Road & Transportation Association, 2005), ribs higher than 150 mm or 200 mm should be applied depending on the placement of tendon. It was more advantageous in terms of deflection to place tendon on the lower part only than to place the lower and upper parts of the section. In addition, we found out that tensile stress which occurs on the top of the section by prestress introduced before the surcharge of live load does not exceed allowable tensile stress. Meanwhile, on Figure 10(a), the values of deflection which tendon is placed on the lower and upper parts are not shown as it is drawn out of range.



(a) Plate thickness: 40mm

(b) Plate thickness: 50mm

(c) Plate thickness: 60mm

Figure 10. Deflection in accordance with rib height

Figure 11 explains how deflection changes according to plate thickness and it varies depending on rib height and tendon placement. When the rib is 100 mm, the deflection decreases as plate thickens and exceeds deflection limit regardless of tendon placement. On the other hand, when the rib height is over 150 mm, the deflection was almost constant regardless of plate thickness except for the case of 40 mm. When tendon was placed only on the lower part, the deflection was within the deflection limit. In the case when tendon was placed on the lower and upper parts of the section, serviceability for deflection was satisfied only when a rib higher than 200 mm was applied.

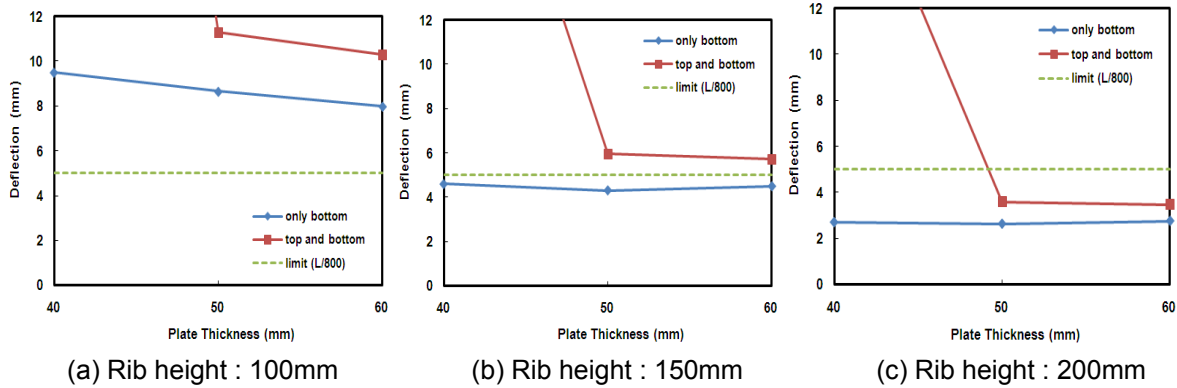


Figure 11. Deflections in accordance with plate thickness

On Figure 12, the number of tendon that is needed on the vertical axis on the left was calculated as 1.1 and 2.0 etc, but we set 2 for every case as an actual number of tendons that can be placed is a whole number. Thus, we were not able to judge economic feasibility of different sections according to the process for prestressing(the number of tendon and the process to introduce prestress).

Meanwhile, on the vertical axis on the right, we demonstrated the concrete volume ratio of UHPC bridge deck slab sections in percentage on consumed quantity of concrete when ordinary prestressed concrete (PSC) bridge deck slab was applied. Here, we assumed a constant size of segment and calculated ordinary PSC slab thickness in accordance with the minimum thickness standards of the KHBDC(2005). Compared with PSC bridge deck slabs, UHPC slab sections were not highly different as they showed a volume ratio range of 26.2% to 29.7% to mark 28.4% average. Assuming that ordinary concrete and UHPC have the same unit weight, the selfweight of UHPC deck slab is below 30% of that of ordinary PSC slab. Therefore, the burden of rising material prices will decrease and additional economic effectiveness will be higher due to the decrease in dead load. In the review of UHPC slab sections, the number of tendon was constant and the volume ratio of concrete was within a similar range.

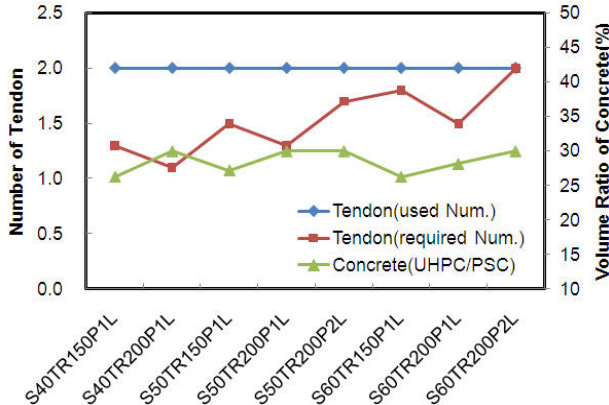


Figure 12. Comparison of UHPC bridge deck slab sections

We compared some sections in this paper (inside the dotted ellipse) with research results or examples of foreign countries as shown on Figure 13. Although slab thickness and rib width do not have any correlation with the slab span, rib height was proportionate to span length.

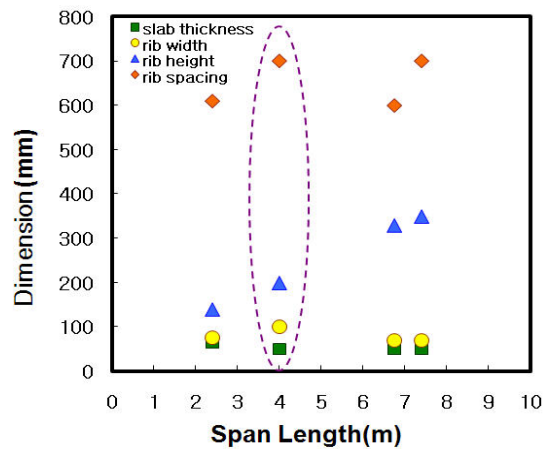


Figure 13. Comparison of specifications of UHPC bridge deck slab section (S50TR200P1L and S50TR200P2L)

3. Conclusion

In this paper, prestressed ribbed type in longitudinal direction was suggested for highly efficient section form of UHPC precast bridge deck slab on a hybrid cable-stayed girder bridge. The followings are conclusions for establishing a concept to design optimal sections.

Plate thickness should be determined at higher than the minimum level to prevent punching shear strength and it does not have a great deal of impact on serviceability for deflection.

Rib spacing should be determined at a level lower than the maximum spacing so as not to induce a two way bending failure on plate members and it varies according to plate thickness.

Rib height is judged to be the most influential variable on efficiency and serviceability for deflection. The minimum rib height that is required to satisfy standard for deflection is affected by the placement of tendon.

Compared with PSC bridge deck slab matching the minimum thickness standards of KHBDC, suggested UHPC precast slab sections show 26%~30% of volume ratio. Presuming the same unit weight, it was assessed that selfweight of deck slab can be reduced to 28% of that of PSC deck slab with ordinary concrete. It can substantively offset the decreased competitiveness of UHPC due to high material prices caused by decreased self-weight of superstructure .

Through static and fatigue tests of UHPC precast bridge deck slab, suggested sectional performance should be verified and later on efficient and reasonable methods to compound segments should be developed. Along with this, methods to composite with cross beam should be designed and a wheel load test to verify the capacity of UHPC precast bridge deck slab system should be conducted.

REFERENCES

1. AASHTO, AASHTO LRFD Bridge Design Specifications 4th, 2007.
2. Korea Road & Transportation Association, Korea Highway Bridges Design Code, Ministry of Land, Transport and Maritime Affairs in Korea, 2005.

3. Korea Concrete Institute, Concrete Structural Design Code, Ministry of Land, Transport and Maritime Affairs in Korea, 2007.
4. F. Toutlemonde, J. Resplendino, L. Sorelli, S. Bouteille, and S. Brisard, "Innovative Design of Ultra High-Performance Fiber Reinforced concrete Ribbed Slab:Experimental Validation and Preliminary Detailed Analyses", Seventh International Symposium on the utilization of High-Strength/High-Performance Concrete, ACI Special Publication SP-228, USA, June, Vol. 2, p.1187-1205.
5. Joh, C. B., Hwang H. H. and Kim, B. S., "Punching Shear and Flexural Strengths of Ultra High Performance Concrete Slabs", Proceedings of HPSM 2008, Algarve, Portugal, 2008.
6. Shaaban, A.M., Gesund, H. (1994), Punching Shear Strength of Steel Fiber Reinforced Concrete Flat Plates. ACI Structural Journal, Vol. 91, No.3, p. 406-414.
7. Spasojevic A, "Structural Implications of Ultra-High Performance Fibre-Reinforced Concrete in Bridge", Ph.D. Thesis, Ecoles Polytechniques Fédérales de Lausanne, Switzerland, 2008